RESEARCH ARTICLE

Metabolite profiling of symbiont and host during thermal stress and bleaching in a model cnidarian–dinoflagellate symbiosis

Katie E. Hillyer[1], Sergey Tumanov[2], Silas Villas-Bôas[3] and Simon K. Davy[1,*]

ABSTRACT

Bleaching (dinoflagellate symbiont loss) is one of the greatest threats facing coral reefs. The functional cnidarian–dinoflagellate symbiosis, which forms coral reefs, is based on the bi-directional exchange of nutrients. During thermal stress this exchange breaks down; however, major gaps remain in our understanding of the roles of free metabolite pools in symbiosis and homeostasis. In this study we applied gas chromatography–mass spectrometry (GC-MS) to explore thermally induced changes in intracellular pools of amino and non-amino organic acids in each partner of the model sea anemone *Aiptasia* sp. and its dinoflagellate symbiont. Elevated temperatures (32°C for 6 days) resulted in symbiont photoinhibition and bleaching. Thermal stress induced distinct changes in the metabolite profiles of both partners, associated with alterations to central metabolism, oxidative state, cell structure, biosynthesis and signalling. Principally, we detected elevated pools of polyunsaturated fatty acids (PUFAs) in the symbiont, indicative of modifications to lipogenesis/lysis, membrane structure and nitrogen assimilation. In contrast, reductions of multiple PUFAs were detected in host pools, indicative of increased metabolism, peroxidation and/or reduced translocation of these groups. Accumulations of glycolysis intermediates were also observed in both partners, associated with photoinhibition and downstream reductions in carbohydrate metabolism. Correspondingly, we detected accumulations of amino acids and intermediate groups in both partners, with roles in gluconeogenesis and acclimation responses to oxidative stress. These data further our understanding of cellular responses to thermal stress in the symbiosis and generate hypotheses relating to the secondary roles of a number of compounds in homeostasis and heat-stress resistance.

KEY WORDS: *Aiptasia*, *Symbiodinium*, Photoinhibition, Coral, GC-MS

INTRODUCTION

The cnidarian–dinoflagellate symbiosis underpins the success of reef-building (scleractinian) corals in nutrient-poor tropical waters (Muscatine and Cernichiari, 1969). In symbioses, dinoflagellate algae of the genus *Symbiodinium* are encapsulated within a host-derived membrane (symbiosome), located within the cnidarian host's gastrodermal cells (Wakefield and Kempf, 2001). This complex partnership (the 'holobiont') may be highly flexible, with a single host associating with multiple *Symbiodinium* clades or sub-clades (types), each with differing physiologies and environmental optima (Baker, 2003). In successful symbioses, there is a complex bi-directional exchange of both organic and inorganic compounds (Muscatine and Hand, 1958; Davy et al., 2012). The photosynthetic symbionts translocate organic products of carbon fixation and nitrogen assimilation to the host, including sugars, sugar alcohols, amino acids and lipids (Gordon and Leggat, 2010; Kopp et al., 2015). In return, the host provides access to dissolved inorganic nutrients (carbon, nitrogen and phosphorus) and may also exchange host-derived amino acids, lipids and fatty acids (Wang and Douglas, 1999; Imbs et al., 2014). The functional holobiont also comprises a specific suite of associated microbial consortia, which are also thought to contribute to these nutritional interactions (Rohwer et al., 2002).

The symbiosis is highly efficient and adapted to relatively wide thermal regimes; however, seawater temperatures are rising and continue to do so, regularly exceeding critical temperature thresholds (Hoegh-Guldberg, 1999). This, in turn, necessitates costly acclimation responses in the symbiont and the host, with a re-organisation of cell metabolism and structure (Kaplan et al., 2004). In symbiosis, this process will occur in each partner individually, but as change is elicited in the downstream exchange of mobile compounds between partners, it will affect the holobiont as a whole (Clark and Jensen, 1982). Acclimation responses will vary according to the holobiont genotype and phenotype; however, they include enzymatic and non-enzymatic antioxidants, photoprotective compounds such as fluorescent proteins and accessory pigments, heat shock proteins, compatible solutes, and structural modifications to maintain cell and organelle stability and function (Lesser, 2006; Baird et al., 2009). Further to their roles in central metabolism, free metabolite pools will function in the *de novo* synthesis of these protective compounds. In addition, they have direct roles as intracellular antioxidants, chelating agents, compatible solutes and cellular signals (Guy et al., 2008; Grüning et al., 2010). Even with costly acclimation responses in place, where elevated temperatures are prolonged and/or severe, thermal stress will lead eventually to dysfunction of the symbiosis, specifically, photoinhibition in the symbiont, the excess production of reactive oxygen species (ROS), and eventually symbiont loss and breakdown, via bleaching (Weis, 2008).

Despite the importance of coral reefs and bleak projections for their future under climate change, major gaps remain in our understanding of how this dynamic and complex symbiosis is affected by high temperature stress and bleaching (Weis, 2008; Davy et al., 2012). In particular, data elucidating changes to mobile compound exchange and downstream pathways in the holobiont are lacking. Less still is known of the secondary roles of many primary metabolites in cellular acclimation, or how these compounds may serve to alter resistance to stress. Metabolomics is a widely used approach for the study of abiotic stressors within clinical research,

[1]School of Biological Sciences, Victoria University of Wellington, PO Box 600, Wellington 6140, New Zealand. [2]Beatson Institute for Cancer Research, Garscube Estate, Switchback Road, Bearsden, Glasgow G61 1BD, UK. [3]Metabolomics Laboratory, School of Biological Sciences, The University of Auckland, Private Bag 92019 Auckland Mail Centre, Auckland 1142, New Zealand.

*Author for correspondence (simon.davy@vuw.ac.nz)

List of symbols and abbreviations

CoA	coenzyme A
FC	fold change
Fd	ferredoxin
FSW	filtered seawater
F_v/F_m	maximum quantum yield of photosystem II
GC-MS	gas chromatography–mass spectrometry
MCF	methyl chloroformate
MUFA	monounsaturated fatty acid
NAD	nicotinamide adenine dinucleotide
NADP/H	nicotinamide adenine dinucleotide phosphate
PAM	pulse amplitude modulated
PAPi	pathway activity profiling
PCA	principal components analysis
PUFA	polyunsaturated fatty acid
ROS	reactive oxygen species
SFA	saturated fatty acid
TCA	tricarboxylic acid

and increasingly in environmental monitoring (Viant, 2008; Lankadurai et al., 2013). Metabolomics refers to the analysis of low molecular weight metabolites within a cell, tissue or biofluid (the 'metabolome') (Viant, 2007). The metabolome of an organism is a downstream product of genotype, phenotype and environmental drivers (Fancy and Rumpel, 2008; Spann et al., 2011). Given a variable of interest, it is therefore possible to detect fine-scale change in a rapid and quantitative manner. Furthermore, by calculating accompanying pathway rate changes, insight can also be gained into wider downstream physiological effects. At the simplest level, one such method for estimating pathway turnover involves the comparison of metabolite abundance and role in particular pathways, producing a hypothetical estimate of pathway activity, which may then be compared between conditions (Aggio et al., 2010). Because of the diversity of the metabolome, no one method is currently capable of capturing all metabolite classes, due to their differing characteristics (Viant, 2008). However, with the application of gas chromatography–mass spectrometry (GC-MS) metabolite profiling, it is possible to simultaneously analyse a relatively large number of metabolite groups in a high throughput, repeatable, sensitive and cost-effective manner (Villas-Bôas et al., 2005).

This study applied GC-MS metabolite profiling and pathway activity analysis to the tropical sea anemone *Aiptasia* sp. and its *in hospite* homologous symbiont (*Symbiodinium minutum*, ITS2 type B1) (Starzak et al., 2014). This anemone is a widely used model system for the study of the cnidarian–dinoflagellate symbiosis (Weis, 2008). The main aim was to investigate heat-stress-induced modifications to the intracellular pools of both partners. Our methods were therefore optimised to focus on pools of amino and non-amino organic acids (in particular, fatty acids). These compounds not only play important roles in the functional metabolism of the holobiont, but have also been previously shown to respond to heat treatment, principally in the maintenance of homeostasis, cell structure, cell signalling and cell death (Díaz-Almeyda et al., 2011; Imbs and Yakovleva, 2012; Leal et al., 2013).

MATERIALS AND METHODS
Specimens of the sea anemone *Aiptasia* sp. were maintained in the laboratory in 1 µm filtered seawater (FSW) at 25°C, with light provided by AQUA-GLO T8 fluorescent bulbs at ≈95 µmol quanta m^{-2} s^{-1} (12 h:12 h light:dark cycle). Anemones were fed twice a week with freshly hatched *Artemia* sp. nauplii. Prior to the experiment, anemones were rinsed repeatedly with FSW to remove

external contaminants. Individuals were acclimated and starved in 25 litre aquaria (light regime as above) for 7 days prior to sampling, to ensure that any *Artemia* nauplii had been digested and expelled. Following acclimation, the treatment aquaria were ramped to 32±0.4°C over a period of 48 h (≈1°C 10 h^{-1}). Once the target temperature was attained, it was maintained for 6 days for the treatment group. A control group was maintained at 25±0.5°C.

Dark-adapted maximum quantum yield of photosystem II (F_v/F_m) was measured with a diving pulse amplitude modulated (PAM) fluorometer (Walz, Effeltrich, Germany), following a 30 min dark adaptation at the end of the daily light cycle. PAM settings were maintained over the course of the experiment at: measuring light 4, saturation intensity 4, saturation width 0.6 s, gain 2 and damping 2. Measurements were taken a standard distance of 5 mm from each sample. Mean estimates with standard error (s.e.m.) were calculated based on single measurements from 10 individuals per treatment at each time point. These same individuals were maintained for daily measurements over the course of the experiment and were not sampled for metabolite profiles.

Sampling for metabolite profiling was undertaken at day 0 (pre-heat ramp) and after 6 days of heat treatment exposure. Three replicate samples were taken at each time point for each treatment. Each individual sample comprised a total of six individuals, to ensure sufficient biomass for metabolite identification (*n*=3×6 anemones per time point and treatment). Individuals for metabolite analysis were immediately quenched by snap-freezing in liquid nitrogen, and were transferred to a −80°C freezer for storage.

Host and *Symbiodinium* separation
Frozen individuals were pooled into single samples and ground with a pestle and mortar, which was chilled with the addition of liquid nitrogen. Once homogenised, 2.4 ml chilled MilliQ water (at 4°C) was added, the sample was thoroughly vortexed, and a 400 µl aliquot was taken for host protein, *Symbiodinium* cell counts and chlorophyll *a* analysis. The remaining homogenate was then centrifuged at 1150 *g* for 5 min at 4°C to pellet the algal symbionts.

The supernatant containing the host fraction was removed, snap-frozen in liquid nitrogen and freeze-dried overnight. The algal pellet was re-suspended in 3 ml chilled MilliQ water and re-centrifuged at 1150 *g* for 5 min at 4°C, and the supernatant discarded. This washing procedure was repeated twice and the resulting algal pellet was freeze-dried overnight. It should be noted that MilliQ water alone was employed for separation and purification phases because of the interaction of buffer precipitates (phosphates) and antifreezes (such as glycerol and ethylene glycol) with the metabolites of interest (K.E.H. and J. Matthews, unpublished data).

Protein quantification, cell counts and chlorophyll *a*
Symbiodinium cell densities were quantified using Improved Neubauer haemocytometer counts (Boeco, Germany), with a minimum of six replicate cell counts per sample (to a confidence interval below 10%). Cell density was normalised to soluble protein content, which was assessed by the Bradford assay (Bradford, 1976) carried out on the supernatant of centrifuged (16,000 *g* for 20 min) host fractions (triplicate measurements). Symbiont chlorophyll *a* content was quantified by dimethylformamide extraction (Moran, 1982) and measured with an ELISA microplate reader (Enspire® 2300, Perkin-Elmer, Waltham, MA, USA) (triplicate measurements).

Extraction
Once dry, 1 ml 50% cold MeOH (at −20°C) was added to each of the samples, which were also spiked with 20 µl of the internal

standard d_4-alanine (at 10 mmol l^{-1}). Methanol-chloroform-washed aluminium beads were added and the samples were vortexed for 1 min, frozen and re-vortexed for a further 1 min. This process was repeated twice for the symbiont samples, to ensure that the cells were fully lysed, identifiable by the orange colour of the extract. Samples were then centrifuged at 3220 *g* for 6 min at −9°C, and the supernatants were collected and stored on dry ice. The extraction was then repeated with the further addition of 1 ml 80% cold MeOH (at −20°C) to the pellet. This second extract was then combined with the first and the pooled sample was freeze-dried overnight. The algal pellet and host cell debris were retained and dried in a drying oven at 100°C, to a constant dry mass.

MCF derivatisation

Derivatisation was via methyl chloroformate (MCF) with the method adapted from Smart et al. (2010). When completely dry, symbiont samples were re-suspended in 200 µl NaOH (1 mol l^{-1}) and transferred to silanised glass tubes (CTS-1275, Thermo Fisher Scientific, USA). After this, a 50 µl aliquot was taken from each sample to produce a pooled sample. To the remaining sample, 167 µl MeOH and 34 µl pyridine were added, followed by 20 µl MCF, and the solution was vortexed for 30 s. A further 20 µl of MCF was then immediately added and the sample was vortexed for another 30 s. Next, 400 µl of chloroform was added to each sample and the mixture was vortexed for 10 s. Finally, 400 µl of sodium bicarbonate (50 mmol l^{-1}) was added and the samples were vortexed for another 10 s. Derivatisation of the host material and production of a pooled sample were as for the symbiont, but all derivatisation volumes were doubled, except in the case of chloroform. Samples were then centrifuged at 1150 *g* for 5 min and the upper aqueous phase was discarded. Any remaining water was then removed from the sample with the addition of sodium sulphate. The remaining extract was then transferred to GC vials for GC-MS analysis.

An isotope-labelled derivative for each metabolite found in the sample was prepared via chemical derivatisation of the pooled sample (algae/host) using isotope-labelled derivatising reagents, namely deuterium-labelled methyl chloroformate (d-MCF) (MT001, Omics, Auckland, New Zealand) and deuterium-labelled methanol (methanol-d_4). A 50 µl aliquot of the relevant d-MCF-derivatised pooled sample (symbiont/host) was then spiked into each of the MCF-derivatised samples prior to GC-MS analysis.

GC-MS analysis

GC-MS was used for identification, semi-quantitation and absolute quantitation of metabolites. This involved use of a Thermo Scientific Trace GC Ultra gas chromatograph coupled to an ISQ mass spectrometer with a programmable temperature vaporising injector.

GC-MS instrument parameters were based on Smart et al. (2010). Briefly, 1 µl of sample was injected using a CTC PAL autosampler into a Siltek™ 2 mm ID straight unpacked inlet liner. The injector was set to 260°C, constant temperature splitless mode with a pressure surge of 180 kPa for 1 min, and column flow of 1.0 ml min^{-1} in constant flow mode. Purge flow was set to 25 ml min^{-1}, 1.2 min after injection.

The column was a fused silica ZB-1701 30 m, with 0.25 mm ID and 0.15 µm film thickness (86% dimethylpolysiloxane, 14% cyanopropylphenyl, Phenomenex). Carrier gas was ultra-high purity grade helium (99.9999%, BOC). GC oven temperature programming started isothermally at 45°C for 2 min, then: increased 9°C min^{-1} to 180°C, held 5 min; increased 40°C min^{-1} to 220°C,

held 5 min; increased 40°C min^{-1} to 240°C, held 11.5 min; and increased 40°C min^{-1} to 280°C, held 2 min. The transfer line to the mass selective detector was maintained at 250°C, and the source at 230°C. The detector was turned on 5.5 min into the run under electron-impact ionisation mode, at 70 eV electron energy, with the electron multiplier set with no additional voltage relative to the autotune value. Solvent blanks were run for every 10–12 samples to monitor instrument carryover. Mass spectra were acquired in scan mode from 38 to 550 AMU, at a rate of 5120 AMU s^{-1}.

Data analysis and validation

Metabolite data extraction and analysis were undertaken based on the protocol described in Smart et al. (2010) with the use of Automated Mass Spectral Deconvolution and Identification System (AMDIS) (http://chemdata.nist.gov/mass-spc/amdis/) and R software, including the packages Metab, Metab-Q and Pathway Activity Profiling (PAPi) (Aggio et al., 2010; Tumanov et al., 2015b), and the software package MetaboAnalyst (Xia et al., 2009, 2012). Compound identification was based on an in-house library of MS spectra. Derivative peak areas were used to semi-quantify the concentrations of individual metabolites in the comparative data set. The comparative data were then normalised to the final area of the internal standard (d_4-alanine) and sample fraction dry mass. For quantitative data, Metab-Q was used to extract abundances of analytes from chromatograms. Metab-Q is in-house software written in the R environment (https://www.r-project.org) that generates a .csv file with individual analyte abundances using an AMDIS report. This script requires the XCMS library (Smith et al., 2006) and can process data files in NetCDF and mzXML formats. Data were then normalised to sample dry mass. Metab-Q is a free software package that can be downloaded from the Metabolomics Laboratory webpage (The University of Auckland, New Zealand; http://metabolomics.auckland.ac.nz/index.php/projects/26).

Data were tested for normality and homogeneity, and transformed where appropriate. IBM SPSS Statistics (v20) was used for both repeated-measures ANOVA (RMANOVA) and ANOVA. RMANOVA was used to test for differences in maximum quantum yields between treatment groups and days (repeat measurements were from the same individuals, which were set aside in each treatment). ANOVA was used to test for differences in heat stress indicators between treatments and sampling days. Statistical significance between the abundance of metabolite treatment means was determined by univariate tests (*t*-test) in MetaboAnalyst. Differences were considered significant at the $P<0.05$ probability level. Fold change analysis was used to compare the absolute value change between group means, before data normalisation was applied. Principal components analysis (PCA) using the normalised, log-transformed and auto-scaled metabolite data was undertaken with MetaboAnalyst. PCA was used to summarise the multivariate metabolite data, capturing the variables that explained the greatest variation [principal components (PC)] in each treatment group. The key-contributing metabolites, as determined by their contribution to the PCA plots, can be identified by their loadings values, as summarised in the corresponding loadings plots.

Pathway activity analysis using the PAPi package was undertaken to compare activities using the normalised and transformed metabolite data following the methods described in Aggio et al. (2010). Briefly, using the normalised abundance data for each treatment at day 6 as input, the PAPi package calculates activity scores of individual pathways from the Kyoto Encyclopedia of Gene and Genomes (KEGG) database. These activity scores are based on the relative changes in compounds (control versus treatment)

associated with each pathway of interest. This algorithm is based on two main assumptions: (1) if a given pathway is active in a cell or organism, more intermediates associated with that pathway will be detected; and (2) during high pathway activity and high turnover, the abundance of associated intermediates will be low. In contrast, during low pathway activity and low turnover, abundance of any associated intermediates will be high (Aggio et al., 2010). The resulting activity score therefore serves as an indicator of the likelihood that a pathway is active within a cell, or organism under a given condition, without the requirement for absolute quantitation such as during more detailed flux analysis. Resulting pathway activity scores were inverted to make interpretation in plotted figures more intuitive, i.e. an increase in activity score representing an increase in the predicted pathway activity. Independent sample t-tests (two-tailed) were used to test for differences between activity scores between treatment groups, with equal variance assumed.

RESULTS

A total of 50 compounds comprising largely amino and non-amino organic acids were identified via GC-MS analysis of the polar and semi-polar extracts of the dinoflagellate (symbiont) and cnidarian (host) fractions. These compounds consisted of 18 amino acids, 11 organic acids and amides, three monounsaturated fatty acids (MUFAs), 12 polyunsaturated fatty acids (PUFAs), five saturated fatty acids (SFAs) and one peptide (Table S1).

Ambient metabolite profiles

Under ambient conditions, symbiont and host profiles differed to a high degree (PC1, 63.1%) in the relative composition of their free metabolite pools (Fig. 1, Table S2). Symbiont profiles were largely composed of a mix of SFAs, MUFA and PUFAs. The most abundant of these – palmitic acid (C16_0), oleic acid (C18_1n) and 11,14,17-eicosatrienoic acid (C20_3n) – were present at concentrations of between 880 and 640 pg μg^{-1} symbiont dry mass. Those distinctive of the symbiont profile included the PUFAs 11,14,17-eicosatrienoic acid (C20_3n), gamma-linolenic acid (C18_3n), 13,16-docosadienoic acid (C22_2n) and 11,14-eicosadienoic acid (C20_2n), and the SFAs myristic acid (C14_0) and dodecanoic acid (C12_0) (Fig. 1).

Host profiles were dominated by a more diverse range of metabolite groups, including SFAs, MUFAs, organic acids and amino acids (Fig. 1, Table S4). The most abundant metabolite was the organic acid citrate, at 3270 pg μg^{-1} host dry mass, followed by the amino acid glutamic acid, the SFA C16_0 and the tripeptide glutathione, which ranged between 1800 and 900 pg μg^{-1} host dry mass. Characteristic metabolites of the host profile included the tripeptide glutathione; the amino acids isoleucine, methionine, cysteine and serine; and the organic acids itaconic acid and citric acid (Fig. 1).

Heat stress indicators

Exposure to 32°C for 6 days resulted in significant declines in F_v/F_m (Fig. S1), which differed with treatment (RMANOVA, time×temperature $F_{6,108}$=12.93, $P<0.001$). After 6 days, F_v/F_m within the treatment group declined ca. 25% to 0.49±0.04, compared with 0.64±0.02 in the control.

Symbiodinium cell density also declined significantly in the heat treatment group (one-way ANOVA, $F_{3,20}$=23.283, $P<0.001$). Elevated temperature treatment caused a 69% reduction in symbiont density after 6 days (from 4.79×10^6±3.42×10^5 to 1.46×10^6±1.55×10^5 cells mg^{-1} protein), while there was no significant decline in the control (Tukey's HSD *post hoc*, P=0.992). Chlorophyll *a* concentration per cell, however, remained unaffected by temperature, with values ranging from approximately 0.82 to 1.21 pg chl *a* cell^{-1} (one-way ANOVA, $F_{3,20}$=1.295, P=0.304).

Heat treatment metabolite profiles

For both symbiont and host, heat treatment caused a shift in metabolite profile, as indicated by the clear separation of the 6-day heat treatment groups within the PCA score plots (Fig. 2). For the symbiont, the heat treatment group was separated along the negative axes of both PC1 and PC2 (PC1, 72.3%, PC2, 11.7%; Fig. 2). For the host fraction, the greatest variance in the data set was accounted for by within-group variability (PC1, 52.7%); heat treatment explained a second level of variance in the data set (PC2, 16.4%; Fig. 2). Metabolite profiles of the 6-day controls and 0-day pre-heat treatment groups closely resembled one another, as reflected in their
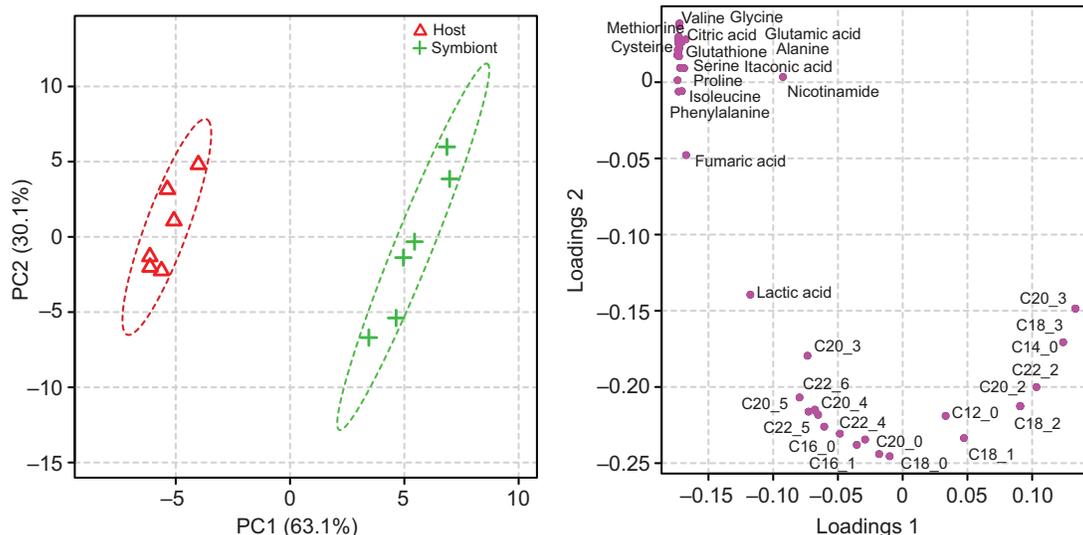

Fig. 1. Characteristics of free metabolite pools in symbiont and host under ambient conditions. Principal components analysis (PCA) scores plot, with 95% confidence intervals (left) and loadings plot (right) of metabolite profile data for dinoflagellate symbiont (symbiont) and cnidarian host samples (host) under ambient conditions.
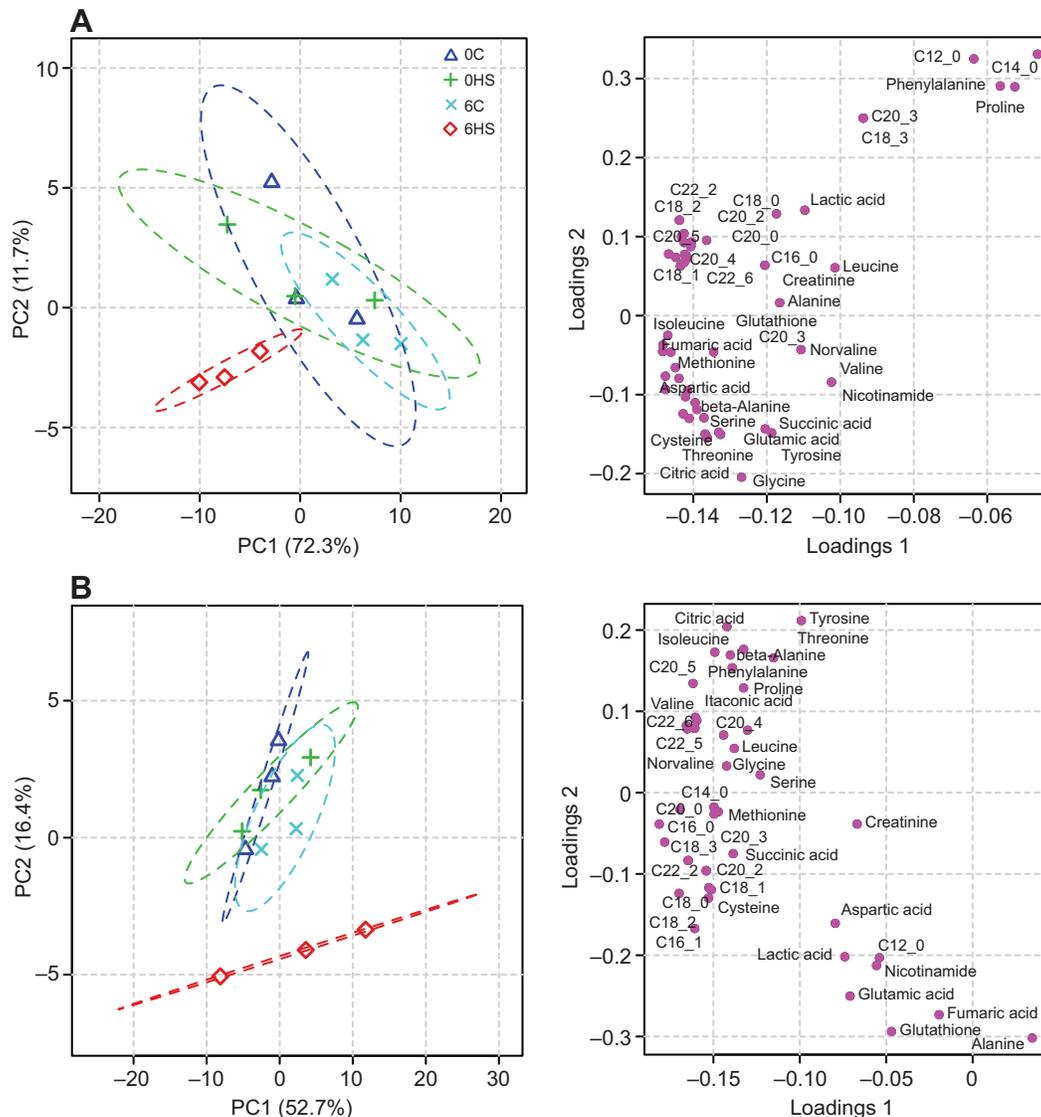
Fig. 2. Change to the composition of free metabolite pools in symbiont and host with thermal stress. (A) Symbiont and (B) host PCA score plots, with 95% confidence intervals (left) and metabolite loadings plots (right). 0C, day 0 control; 0HS, day 0 heat stress; 6C, day 6 control; 6HS, day 6 heat stress.

similar PC scores and the spatial overlap of these groups in the PCA score plots.

Heat-responsive metabolites in the symbiont
The metabolites contributing the most to the heat treatment effect in the symbiont metabolite pools are summarised in Fig. 3. Briefly, they include the organic acid succinate and the amino acids valine, norvaline, threonine and methionine (Fig. 3). Those typical of the control included the SFAs myristic acid (C14_0) and dodecanoic acid (C12_0).

With respect to quantitative data of individual compounds, we detected significant concentration increases and fold changes for multiple metabolite groups (Table S3). Notably, the organic acids lactate, fumarate, citrate and succinate, the amino acids glycine, beta-alanine, threonine, valine, norvaline and methionine, and the PUFAs alpha- and gamma-linolenic acid (C18_3n) and 11,14,17-eicosatrienoic acid (C20_3n) (Fig. 4).

As a result of these relative alterations in pools between ambient and heat-stress groups, we estimated multiple activity changes to downstream networks, especially those associated with central metabolism, fatty acid metabolism and cellular homeostasis (Fig. 5). Principally, we estimated activity reductions for pathways associated with glycolysis, oxidative phosphorylation and the tricarboxylic acid (TCA) cycle. Coupled to these modifications to central metabolism, we estimated declines in the activity of biosynthesis pathways for a number of amino acids and fatty acids. We also estimated a reduction in the on-going metabolism of a number of amino acids and cellular antioxidants, including glutathione and nicotinamide, associated with their accumulation during thermal stress.

Heat-responsive metabolites in the host
Key metabolites that contributed to the metabolite profile of thermally stressed anemone tissues included the SFA dodecanoic acid (C12_0), the nucleotide precursor nicotinamide, the tripeptide glutathione, and the organic acids lactate and fumarate (Fig. 3). Similarly, we detected significant concentration increases and fold changes for the same compounds, in addition to the amino acids alanine and glutamic acid (Table S4).
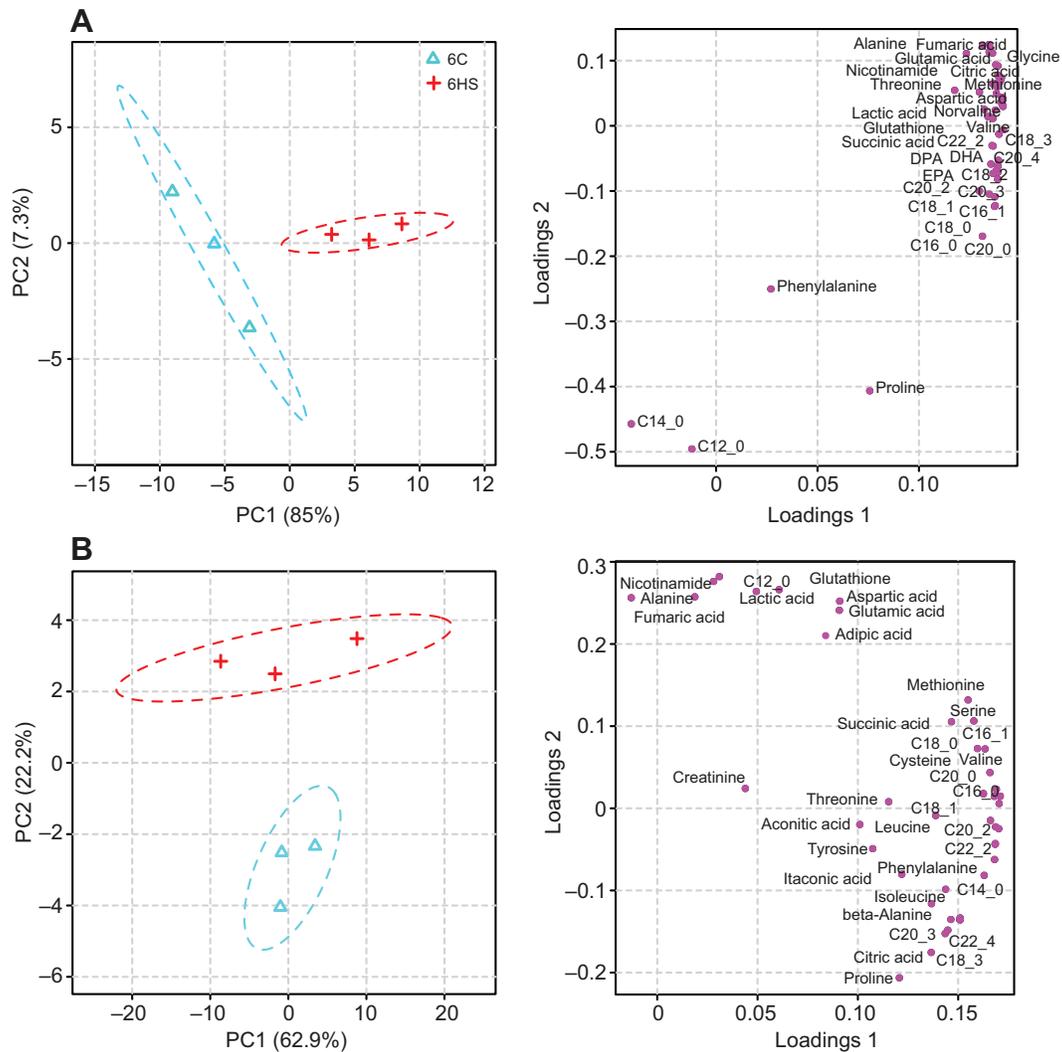
Fig. 3. Change to the composition of free metabolite pools of symbiont and host at 6 days of thermal stress. (A) Symbiont and (B) host PCA score plots, with 95% confidence intervals (left) and metabolite loadings plots (right). 6C, day 6 control; 6HS, day 6 heat stress.

Alterations to pathway turnover were estimated for a number of central and homeostatic networks as a result of temperature treatment (Fig. 5). Briefly, we estimated relative increases in pathways linked to the generation of energy via gluconeogenesis, namely the TCA cycle, coenzyme A (CoA) biosynthesis and oxidative phosphorylation, coupled to declines in glycolysis and pyruvate metabolism. These alterations coincided with increased activity of the metabolism of a number of fatty acids and amino acids. We also detected increased activity of networks associated with lipid signalling pathways, namely, those associated with the oxidation of the fatty acids arachidonic acid (C20_4) and linoleic acid (C18_2). Correspondingly, we estimated reduced metabolism of cellular antioxidants, including glutathione and thiol-containing amino acids, associated with their accumulation with thermal stress.

DISCUSSION

This study characterised metabolite profiles, in both partners of a model cnidarian–dinoflagellate symbiosis, during ambient conditions and following exposure to elevated temperature. Heat treatment (32°C for 6 days) resulted in thermal stress and breakdown of the symbiosis (bleaching). We observed marked, thermally induced changes in the pools of intracellular free

metabolites in both partners. Associated with these modifications, we identified alterations to the activities of central metabolic pathways, such as glycolysis and gluconeogenesis, in addition to those associated with nitrogen assimilation, biosynthesis, cellular homeostasis and cell signalling (Fig. 6).

Changes to specific metabolite groups and pathways in response to heat stress
Fatty acids

Fatty acids and lipids are synthesised *de novo* by ligation of acetyl-CoA, via the action of elongase enzymes (Tumanov et al., 2015a). Synthesis pathways vary between species, and autotrophic and heterotrophic organisms have different abilities to produce specific fatty acid groups (Dunn et al., 2012; Leal et al., 2013). Fatty acids and lipids play major roles in the functional cnidarian–dinoflagellate symbiosis, acting directly in the primary metabolism of both partners and mobile compound exchange between partners (Dunn et al., 2012; Imbs et al., 2014; Kopp et al., 2015). As major energy stores in the dinoflagellate symbiont, lipid and fatty acid pools are also indicative of carbon to nitrogen (C:N) ratios, cell proliferation and the status of on-going nitrogen assimilation (Wang et al., 2013; Jiang et al., 2014) (Fig. 6). Free
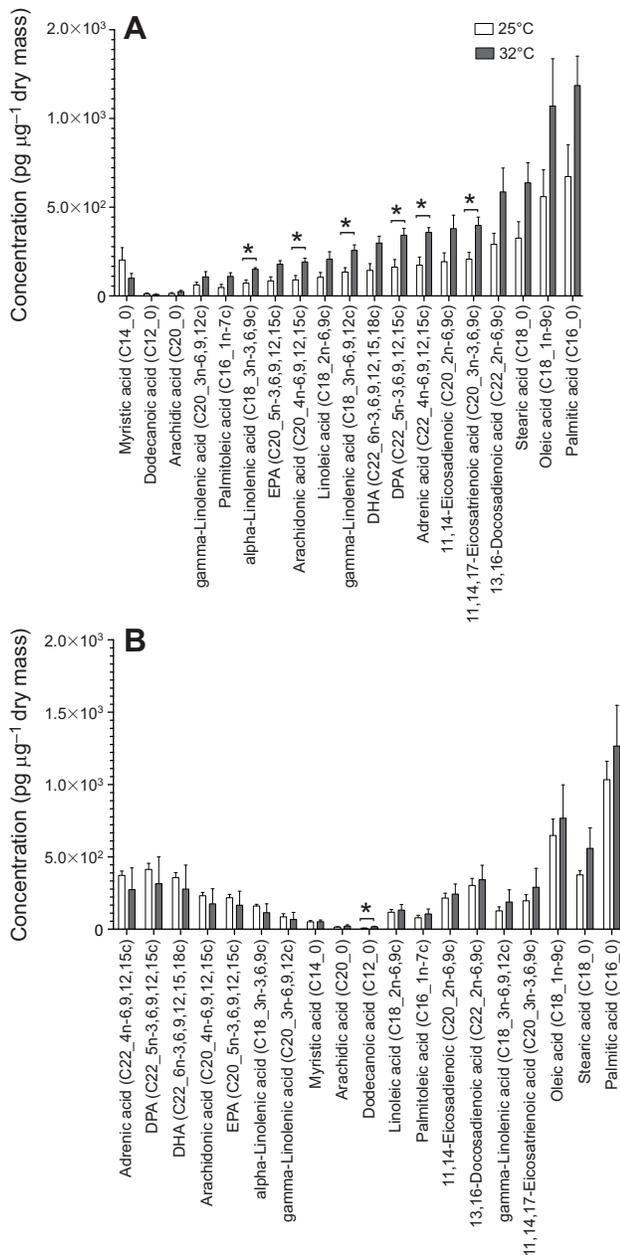
Fig. 4. Free fatty acid concentrations in symbiont and host pools under ambient conditions and thermal stress. Concentration of individual compounds in (A) symbiont and (B) host free fatty acid pools per µg dry mass during ambient conditions (25°C) and following exposure to thermal stress (32°C for 6 days) from the anemone *Aiptasia* sp. *t*-test concentration×treatment. Asterisks indicate a significant difference between treatments (*$P<0.05$).

fatty acid pools also function in cellular homeostasis, with highly conserved roles in membrane structure, function and cell signalling (Díaz-Almeyda et al., 2011; Dunn et al., 2012). Correspondingly, in the present study we detected a high diversity and abundance of free SFAs, MUFAs and PUFAs in the free fatty acid pools of both partners, in ambient and heat-stressed conditions. Under ambient conditions, many of these compounds were found at relatively high abundances in both partners (C16_0, C18_0, C18_1), although the relative contributions of individual compounds differed in each partner (e.g. C22_2:C22_5 ratio). We also detected multiple fatty acids (primarily DHA, C22_6n) in host pools that are characteristic of the mobile products of the dinoflagellate symbionts (Dunn et al.,

2012; Kneeland et al., 2013), and vice versa (DPA, C22_5n) (Imbs et al., 2014).

Photoinhibition of the symbiont, as indicated by a large reduction (ca. 25%) in F_v/F_m, will result in a net reduction in the generation of cellular energy (ATP and NADPH) and an increase in ROS production (Smith et al., 2005). This will impact the fatty acid pools of both symbiont and host in a number of complex ways.

For example, there will be a shift in metabolic modes to those that generate, rather than consume, ATP. One such important mechanism for energy generation is gluconeogenesis, where energy stores are catabolised to produce ATP. Lipids are broken down via beta-oxidation to produce acetyl-CoA, which is in turn fed into the TCA cycle, generating ATP (Grottoli and Rodrigues, 2011; Imbs and Yakovleva, 2012) (see 'Organic acids, intermediates and antioxidants', below). Although we did not analyse total lipids, which comprise the entirety of lipid stores, free pools of polar and semi-polar fatty acids comprise a major fraction of these stores (Imbs and Yakovleva, 2012; Jiang et al., 2014). Associated with photoinhibition and this energy deficit, we detected a negative trend in pools of a number of SFAs in the symbiont (C12_0 and C14_0). These relative reductions may be indicative of increased turnover and/or a decline in fatty acid elongation and lipogenesis in the heat-stressed symbiont.

A decline in *de novo* lipogenesis pathways, which consume ATP, and a reduction in downstream translocation of these mobile products to the host would also be expected under thermal stress and photoinhibition (Papina et al., 2007; Imbs and Yakovleva, 2012) (Fig. 6). Correspondingly, we detected accumulations of multiple long-chain PUFA intermediates in symbiont FA pools. Concomitantly, in host pools we detected reductions of multiple long-chain PUFAs, which are considered characteristic of symbiont-derived mobile products (such as DHA) (Papina et al., 2003; Kneeland et al., 2013). In the host we also estimated a trend of increased activity of the TCA cycle and the production of acetyl-CoA, consistent with a decline in mobile product translocation and an increase in the activity of this energy-generating network (Papina et al., 2007; Imbs and Yakovleva, 2012). An additional explanation for the observed accumulations in symbiont pools, is translocation of host-derived PUFAs (Imbs et al., 2014). Host-derived compounds include the long-chain PUFAs DPA (C22_5n) and linoleic acid (C18_2n), and the SFA arachidic acid (C20_0), all of which were also detected in symbiont pools in the present study. Interestingly, symbiont pools of DPA were also elevated with thermal stress, indicative of a reduction in its metabolism and/or increased translocation of this compound during thermal stress.

A reduction in photosynthesis will also necessitate an alternative sink for electrons in the chloroplasts of the dinoflagellate; the major mechanism in *Symbiodinium* is via the Mehler reaction (Reynolds et al., 2008). This pathway, in turn, produces high levels of cellular ROS, in the form of relatively persistent hydrogen peroxide, which can result in damage to the lipid bilayer of cell membranes (Tchernov et al., 2004). PUFAs in particular are considered sensitive to both peroxidation and photo-oxidation (Tchernov et al., 2004; Papina et al., 2007). During prolonged oxidative stress, where antioxidant responses are overwhelmed, there will be increased oxidation of PUFAs to oxylipins, which are highly unstable and result in further damage (Gill and Tuteja, 2010). As a result, many oxylipins function as conserved messenger molecules in stress signalling, programmed cell death and defence responses (Savchenko et al., 2010). More specifically, the eicosanoid pathway (of which C20_4 is a major substrate) functions in this stress-signalling cascade, a process also recently described in the soft coral
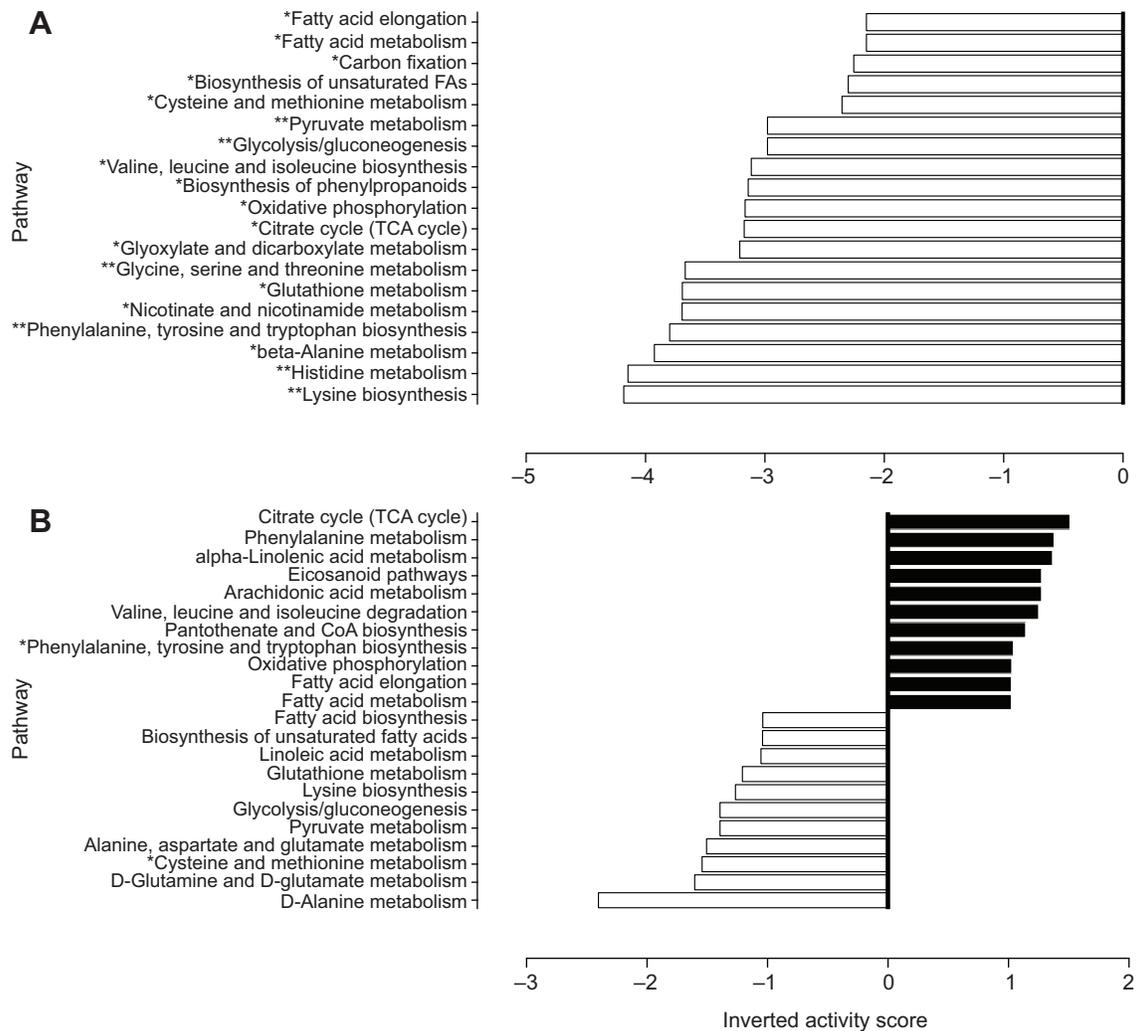
Fig. 5. Pathway activity fold changes in symbiont and host associated with exposure to 6 days of thermal stress. Relative change in key (A) symbiont and (B) host metabolite pathway activities following 6 days of heat stress at 32°C (PAPi activity analysis, 6-day control versus 6-day heat treatment, t-test activity score×treatment, two-tailed). Asterisks indicate a significant difference between treatments at day 6 (**$P<0.005$, *$P<0.05$).

Capnella imbricata (Lõhelaid et al., 2015). The observed reductions of C20 PUFAs in host pools can therefore be considered indicative of prolonged oxidative stress and highlight the possibility that oxylipin-based signalling cascades may also operate in *Aiptasia*.

Increased saturation of the cell lipid bilayer functions in thermal acclimation directly and indirectly, by increasing stability and protecting it against damage by ROS (Pearcy, 1978; Tchernov et al., 2004; Papina et al., 2007). We detected a positive trend in the pools of the major SFAs C16_0 and C18_0, in addition to C18_1 in both partners. However, with our methods it was not possible to establish whether these changes were associated with modifications to cell membranes, or were simply a reflection of altered fatty acid metabolism, or a combination of the two. However, increasing membrane saturation is energetically costly, consuming ATP to break and re-form lipid structures; it may also be dependent on cell type (Díaz-Almeyda et al., 2011). In contrast, relatively thermally resistant *Symbiodinium* types may actively increase pools of PUFAs (Díaz-Almeyda et al., 2011). As the process of fatty acid desaturation is also in itself an aerobic reaction, desaturation, elongation and isomerisation may simultaneously reduce cellular oxidative stress, increase melting points and reduce peroxidation, thereby providing an additional mechanism for membrane

stabilisation (Guerzoni et al., 2001; Díaz-Almeyda et al., 2011). However, as PUFAs are in themselves susceptible to peroxidation by ROS, this response will only be effective as long as antioxidant responses are maintained. In agreement with Díaz-Almeyda et al. (2011), we detected elevated pools of multiple PUFAs in the symbiont following exposure to thermal stress. The homologous *Symbiodinium* type in the present study (B1) is considered moderately robust to thermal and oxidative stress (Wietheger et al., 2015), and a similar mechanism may therefore operate in this symbiont. This process of PUFA accumulation is also common in dinoflagellates under nitrogen limitation as C:N ratios become elevated, and may therefore also be indicative of reductions in nitrogen assimilation (see 'Amino acids', below) (Jiang et al., 2014; Wang et al., 2015).

Amino acids

Amino acid pools not only function in biosynthesis, growth and respiration via gluconeogenesis, but their exchange as mobile compounds is also thought to play a role in maintaining the functional symbiosis (Livingstone, 1991; Wang and Douglas, 1999; Butterfield et al., 2013). Inorganic nitrogen is directly assimilated in both symbiont and host from ammonium and nitrate (Pernice et al.,
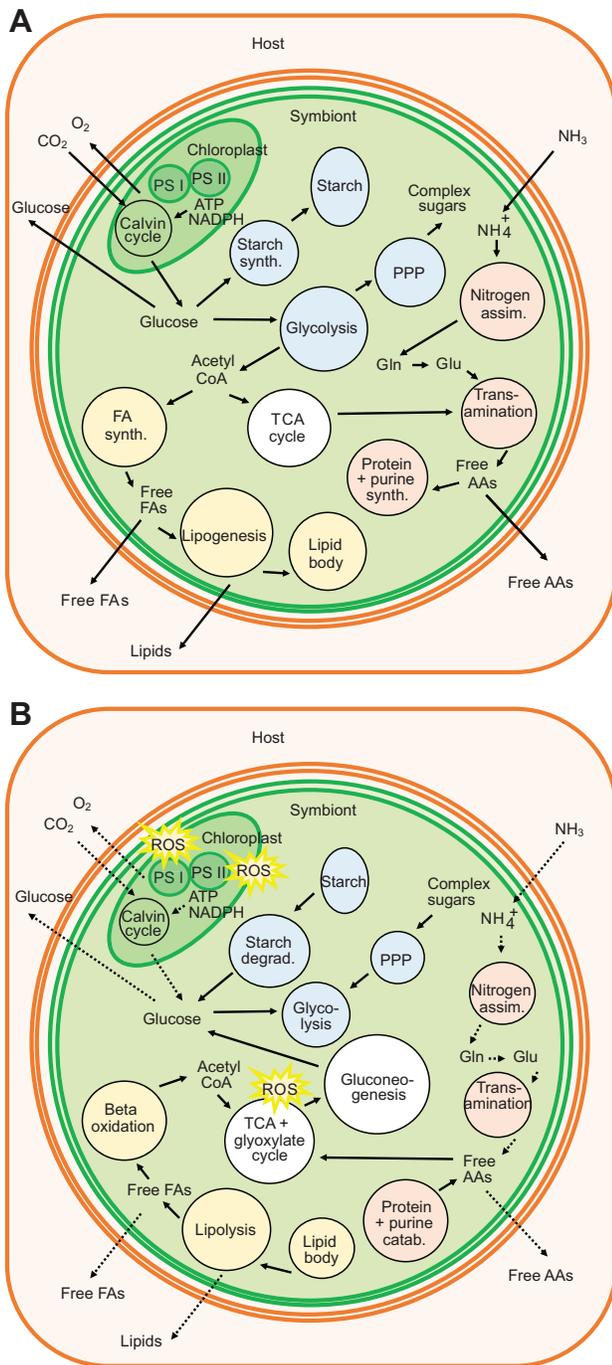
Fig. 6. Simplified summary of the major metabolic pathways in the symbiont under functional photosynthetic conditions and potential changes during thermal stress. (A) Major metabolic pathways in the dinoflagellate symbiont during photosynthetic conditions and functional symbiosis and (B) potential modifications during thermal stress and photoinhibition. Dotted lines denote a reduction in associated pathway activity. AA, amino acid; CoA, coenzyme A; FA, fatty acid; PPP, pentose phosphate pathway; PS I/II, photosystem I/II; ROS, reactive oxygen species; TCA, tricarboxylic acid. These pathways will occur throughout numerous cell organelles (including the chloroplast); however, for clarity only photosynthesis is displayed in the chloroplast.

2012). However, nitrate must first be reduced by nitrate reductase, a process using reduced ferredoxins (Fd) from the photosynthetic transport chain, or NAD(P)H (in non-photosynthetic organisms)

(Dagenais-Bellefeuille and Morse, 2013). Ammonium is then assimilated via the glutamine synthetase/glutamine:2-oxoglutarate aminotransferase cycle (Pernice et al., 2012). In this cycle, ammonium is added to glutamine (Gln) to produce glutamate (Glu), consuming ATP, Glu is then reduced back to Gln with either reduced-Fd or NAD(P)H (Dagenais-Bellefeuille and Morse, 2013). The abundance of Glu and Gln can therefore serve as a sensitive indicator of nitrogen assimilation in the symbiosis (Pernice et al., 2012) (Fig. 6). The capacity to assimilate nitrogen in this way is present in both symbiont and host, but the process is much more rapid in the dinoflagellate (Swanson and Hoegh-Guldberg, 1998; Pernice et al., 2012). Following assimilation by the symbiont, synthesised amino acids will therefore have a number of fates, where they may be: (1) used in the production of other amino acids and proteins; (2) directly metabolised via the TCA cycle (see 'Organic acids, intermediates and antioxidants', below); (3) translocated to the host; or (4) metabolised in the purine pathway (Wang and Douglas, 1999; Pernice et al., 2012).

Thermal stress resulted in a number of changes to the amino acid pools of both symbiont and host, reflecting modifications to the activity of nitrogen assimilation and the downstream fate of assimilated compounds. Firstly, Glu accumulated in symbiont pools (and to a lesser extent in pools of the host). As nitrogen assimilation consumes ATP and requires reduced-Fd, photoinhibition is likely to result in a decline in the activity of this process, with the accumulation of the non-reduced intermediate Glu in symbiont pools as a result. Secondly, we also detected accumulations in symbiont pools of numerous other amino acid groups; these included isoleucine and valine, which, under functional conditions, are thought to be synthesised by the symbiont and translocated to the host (Wang and Douglas, 1999). Accumulations of these amino acids are therefore once again likely to be indicative of a reduction in the activity of ATP-consuming biosynthesis pathways, such as transamination and protein synthesis and of declines in downstream mobile product translocation to the host, coupled to increases in ATP-generating pathways such as the breakdown of proteins during gluconeogenesis (Wang and Douglas, 1998; Whitehead and Douglas, 2003).

Of note was the accumulation of thiols, or the sulphur-containing amino acids cysteine and methionine, in the symbiont pools with heat stress. This group has a number of highly conserved secondary functions, which include acting as ROS scavengers and redox sensors (Mayer et al., 1990), and may therefore perform a similar function in the symbiont under thermal and oxidative stress.

Organic acids, intermediates and antioxidants
Organic acids and pathway intermediates play essential roles in central metabolic pathways, including the TCA cycle, glycolysis, oxidative phosphorylation, the pentose phosphate pathway and gluconeogenesis (Livingstone, 1991; Ganot et al., 2011; Butterfield et al., 2013). They also have important functions in the production of co-enzymes and antioxidants, and as signalling molecules (Krüger et al., 2011). Heat treatment induced changes in these pools in both partners of the symbiosis. Most notably, we observed increases of intermediates linked principally to glycolytic pathways and pyruvate metabolism, in both symbiont and host. In glycolysis, glucose is broken down into pyruvate, which is eventually fed into the TCA cycle to generate energy (ATP) (Fernie et al., 2004). In the symbiont, reductions in pathway activities linked to modes of carbohydrate metabolism are likely to reflect the downstream results of photoinhibition (Lesser, 1997). Declines in the host would further imply that, under heat stress,

carbohydrate pools were also diminished, most likely because of reduced translocation from the symbiont (Clark and Jensen, 1982; Loram et al., 2007) (Fig. 6).

However, in the host fraction we also detected reductions in pools of intermediates linked to other aspects of central metabolism, namely the TCA cycle and oxidative phosphorylation, suggesting increased turnover of these networks. These shifts are likely due to the ongoing energetic costs associated with maintaining homeostasis under elevated temperature, such as modifications to the structure of cell membranes, which in turn necessitate the generation of energy from alternate pathway modes (as discussed above) (Coles and Jokiel, 1977; Clark and Jensen, 1982), such as via gluconeogenesis and beta-oxidation, in the breakdown of proteins and lipids (Lehnert et al., 2014).

Also of note was the accumulation of nicotinamide in both partners. This compound is the precursor to the essential coenzymes nicotinamide adenine dinucleotide (NAD) and nicotinamide adenine dinucleotide phosphate (NADP). These coenzymes facilitate many oxidation and reduction reactions in living cells, which include linking the TCA cycle and oxidative phosphorylation (Berglund and Ohlsson, 1995). In *Symbiodinium*, as in other primary producers, NADP$^+$ is a major acceptor of electrons in photosystem I, which in turn reduces the production of ROS (Takahashi and Murata, 2008). In higher plants, nicotinamide has been identified as a signal molecule of DNA damage and oxidative stress, which facilitates a number of defence-related metabolic reactions (Berglund, 1994; Berglund and Ohlsson, 1995). A similar defence and signalling mechanism may also function in the cnidarian–dinoflagellate symbiosis, though this awaits confirmation. In addition, pools of the antioxidant compound glutathione were elevated in both partners. Glutathione is a tripeptide antioxidant that serves as an important electron donor during oxidative stress in *Symbiodinium* (Lesser, 2006; Krueger et al., 2014) and in the cnidarian host (Downs et al., 2002; Desalvo et al., 2008; Sunagawa et al., 2008), consistent with the findings of the present study.

Conclusions

Free metabolite pools and mobile compound exchange between symbiotic partners are essential to the functional cnidarian–dinoflagellate symbiosis. Primary metabolites function directly in central metabolism, and in cellular acclimation and homeostasis. Prolonged exposure to elevated temperatures above critical temperature thresholds results in symbiont photoinhibition, bleaching and distinct changes in the metabolite profiles of both symbiont and host. These modifications are associated with declines in carbon fixation, altered metabolic mode, declines in mobile product translocation, and acclimation responses to thermal and oxidative stress. These data provide further insight into the differing cellular responses of symbiont and host to these abiotic stressors during bleaching in a model system for reef-building corals. The outputs of this study also highlight a number of gaps in knowledge that warrant further study, for instance, the roles of free metabolite pools in stress-signalling cascades and signal transduction, within and between partners, are largely undescribed in the symbiosis. This study also highlights the need for further investigation into the central metabolic networks of both partners of the symbiosis, where major gaps still remain.

The application of metabolomics to coral reef studies

Clearly a major strength of metabolomics-based techniques lies in the capacity to simultaneously detect subtle changes in a large variety of small compounds, with little *a priori* knowledge of the metabolite pools under investigation. As these pools have important and conserved roles in respiration, growth, cellular homeostasis and signalling, quantitative insight can be gained into the activity of these networks. However, in many cases direct evidence from the cnidarian–dinoflagellate symbiosis is still lacking and further targeted studies are therefore required to test the roles of many compounds in the cellular responses of both partners. For instance, a more in-depth understanding of the cell-signalling network is essential if we are to better understand how the holobiont detects, communicates and responds to stress. These data may also prove useful in the development of metabolite markers of thermal and other abiotic stressors that can be used for monitoring of the symbiosis and of coral reef systems. Further studies that apply high-resolution visualisation of metabolite pools, such as nanoscale secondary ion mass spectrometry (NanoSIMS), coupled with stable isotope tracers will serve to provide further insight into the potential roles of free metabolites in differing compartments of the holobiont. These data, coupled with the on-going outputs from rapidly developing 'omics' studies (genomics, transcriptomics, proteomics and metabolomics) will aid in further elucidating the metabolic cross-talk both within and between partners, which is essential for maintaining the functional holobiont.

References

Aggio, R. B. M., Ruggiero, K. and Villas-Bôas, S. G. (2010). Pathway Activity Profiling (PAPi): from the metabolite profile to the metabolic pathway activity. *Bioinformatics* **26**, 2969-2976.

Baird, A. H., Bhagooli, R., Ralph, P. J. and Takahashi, S. (2009). Coral bleaching: the role of the host. *Trends Ecol. Evol.* **24**, 16-20.

Baker, A. C. (2003). Flexibility and specificity in coral–algal symbiosis: diversity, ecology, and biogeography of *Symbiodinium. Annu. Rev. Ecol. Evol. Syst.* **34**, 661-689.

Berglund, T. (1994). Nicotinamide, a missing link in the early stress response in eukaryotic cells: a hypothesis with special reference to oxidative stress in plants. *FEBS Lett.* **351**, 145-149.

Berglund, T. and Ohlsson, A. (1995). Defensive and secondary metabolism in plant tissue cultures, with special reference to nicotinamide, glutathione and oxidative stress. *Plant Cell Tissue Organ Cult.* **43**, 137-145.

Bradford, M. M. (1976). A rapid and sensitive method for the quantitation of microgram quantities of protein utilizing the principle of protein-dye binding. *Anal. Biochem.* **72**, 248-254.

Butterfield, E. R., Howe, C. J. and Nisbet, R. E. R. (2013). An analysis of dinoflagellate metabolism using EST data. *Protist* **164**, 218-236.

Clark, K. B. and Jensen, K. R. (1982). Effects of temperature on carbon fixation and carbon budget partitioning in the zooxanthellal symbiosis of *Aiptasia pallida* (Verrill). *J. Exp. Mar. Biol. Ecol.* **64**, 215-230.

Coles, S. L. and Jokiel, P. L. (1977). Effects of temperature on photosynthesis and respiration in hermatypic corals. *Mar. Biol.* **43**, 209-216.

Dagenais-Bellefeuille, S. and Morse, D. (2013). Putting the N in dinoflagellates. *Front. Microbiol.* **4**, 369.

Davy, S. K., Allemand, D. and Weis, V. M. (2012). Cell biology of cnidarian–dinoflagellate symbiosis. *Microbiol. Mol. Biol. Rev.* **76**, 229-261.

Desalvo, M. K., Voolstra, C. R., Sunagawa, S., Schwarz, J. A., Stillman, J. H., Coffroth, M. A., Szmant, A. M. and Medina, M. (2008). Differential gene expression during thermal stress and bleaching in the Caribbean coral *Montastraea faveolata*. *Mol. Ecol.* **17**, 3952-3971.

Díaz-Almeyda, E., Thomé, P. E., El Hafidi, M. and Iglesias-Prieto, R. (2011). Differential stability of photosynthetic membranes and fatty acid composition at elevated temperature in *Symbiodinium*. *Coral Reefs* **30**, 217-225.

Downs, C. A., Fauth, J. E., Halas, J. C., Dustan, P., Bemiss, J. and Woodley, C. M. (2002). Oxidative stress and seasonal coral bleaching. *Free Radic. Biol. Med.* **33**, 533-543.

Dunn, S. R., Thomas, M. C., Nette, G. W. and Dove, S. G. (2012). A lipidomic approach to understanding free fatty acid lipogenesis derived from dissolved inorganic carbon within cnidarian–dinoflagellate symbiosis. *PLoS ONE* **7**, e46801.

Fancy, S.-A. and Rumpel, K. (2008). GC-MS-based metabolomics. In *Biomarker Methods in Drug Discovery and Development* (ed. F. Wang), pp. 317-340. New York: Humana Press.

Fernie, A. R., Carrari, F. and Sweetlove, L. J. (2004). Respiratory metabolism: glycolysis, the TCA cycle and mitochondrial electron transport. *Curr. Opin. Plant Biol.* **7**, 254-261.

Ganot, P., Moya, A., Magnone, V., Allemand, D., Furla, P. and Sabourault, C. (2011). Adaptations to endosymbiosis in a cnidarian–dinoflagellate association: differential gene expression and specific gene duplications. *PLoS Genet.* **7**, e1002187.

Gill, S. S. and Tuteja, N. (2010). Reactive oxygen species and antioxidant machinery in abiotic stress tolerance in crop plants. *Plant Physiol. Biochem.* **48**, 909-930.

Gordon, B. R. and Leggat, W. (2010). *Symbiodinium*–invertebrate symbioses and the role of metabolomics. *Mar. Drugs* **8**, 2546-2568.

Grottoli, A. G. and Rodrigues, L. J. (2011). Bleached *Porites compressa* and *Montipora capitata* corals catabolize δ^{13}C-enriched lipids. *Coral Reefs* **30**, 687-692.

Grüning, N.-M., Lehrach, H. and Ralser, M. (2010). Regulatory crosstalk of the metabolic network. *Trends Biochem. Sci.* **35**, 220-227.

Guerzoni, M. E., Lanciotti, R. and Cocconcelli, P. S. (2001). Alteration in cellular fatty acid composition as a response to salt, acid, oxidative and thermal stresses in *Lactobacillus helveticus*. *Microbiology* **147**, 2255-2264.

Guy, C., Kaplan, F., Kopka, J., Selbig, J. and Hincha, D. K. (2008). Metabolomics of temperature stress. *Physiol. Plant.* **132**, 220-235.

Hoegh-Guldberg, O. (1999). Climate change, coral bleaching and the future of the world's coral reefs. *Mar. Freshw. Res.* **50**, 839-866.

Imbs, A. B. and Yakovleva, I. M. (2012). Dynamics of lipid and fatty acid composition of shallow-water corals under thermal stress: an experimental approach. *Coral Reefs* **31**, 41-53.

Imbs, A. B., Yakovleva, I. M., Dautova, T. N., Bui, L. H. and Jones, P. (2014). Diversity of fatty acid composition of symbiotic dinoflagellates in corals: evidence for the transfer of host PUFAs to the symbionts. *Phytochemistry* **101**, 76-82.

Jiang, P.-L., Pasaribu, B. and Chen, C.-S. (2014). Nitrogen-deprivation elevates lipid levels in *Symbiodinium* spp. by lipid droplet accumulation: morphological and compositional analyses. *PLoS ONE* **9**, e87416.

Kaplan, F., Kopka, J., Haskell, D. W., Zhao, W., Schiller, K. C., Gatzke, N., Sung, D. Y. and Guy, C. L. (2004). Exploring the temperature-stress metabolome of *Arabidopsis*. *Plant Physiol.* **136**, 4159-4168.

Kneeland, J., Hughen, K., Cervino, J., Hauff, B. and Eglinton, T. (2013). Lipid biomarkers in *Symbiodinium* dinoflagellates: new indicators of thermal stress. *Coral Reefs* **32**, 923-934.

Kopp, C., Domart-Coulon, I., Escrig, S., Humbel, B. M., Hignette, M. and Meibom, A. (2015). Subcellular investigation of photosynthesis-driven carbon assimilation in the symbiotic reef coral *Pocillopora damicornis*. *MBio* **6**, e02299-14.

Krueger, T., Becker, S., Pontasch, S., Dove, S., Hoegh-Guldberg, O., Leggat, W., Fisher, P. L. and Davy, S. K. (2014). Antioxidant plasticity and thermal sensitivity in four types of *Symbiodinium* sp. *J. Phycol.* **50**, 1035-1047.

Krüger, A., Grüning, N.-M., Wamelink, M. M. C., Kerick, M., Kirpy, A., Parkhomchuk, D., Bluemlein, K., Schweiger, M.-R., Soldatov, A., Lehrach, H. et al. (2011). The pentose phosphate pathway is a metabolic redox sensor and regulates transcription during the antioxidant response. *Antioxid. Redox Signal.* **15**, 311-324.

Lankadurai, B. P., Nagato, E. G. and Simpson, M. J. (2013). Environmental metabolomics: an emerging approach to study organism responses to environmental stressors. *Environ. Rev.* **21**, 180-205.

Leal, M. C., Nunes, C., Kempf, S., Reis, A., da Silva, T. L., Serôdio, J., Cleary, D. F. R. and Calado, R. (2013). Effect of light, temperature and diet on the fatty acid profile of the tropical sea anemone *Aiptasia pallida*. *Aquacult. Nutr.* **19**, 818-826.

Lehnert, E. M., Mouchka, M. E., Burriesci, M. S., Gallo, N. D., Schwarz, J. A. and Pringle, J. R. (2014). Extensive differences in gene expression between symbiotic and aposymbiotic cnidarians. *G3* **4**, 277-295.

Lesser, M. P. (1997). Oxidative stress causes coral bleaching during exposure to elevated temperatures. *Coral Reefs* **16**, 187-192.

Lesser, M. P. (2006). Oxidative stress in marine environments: biochemistry and physiological ecology. *Annu. Rev. Physiol.* **68**, 253-278.

Livingstone, D. R. (1991). Origins and evolution of pathways of anaerobic metabolism in the animal kingdom. *Am. Zool.* **31**, 522-534.

Lõhelaid, H., Teder, T. and Samel, N. (2015). Lipoxygenase-allene oxide synthase pathway in octocoral thermal stress response. *Coral Reefs* **34**, 143-154.

Loram, J. E., Trapido-Rosenthal, H. G. and Douglas, A. E. (2007). Functional significance of genetically different symbiotic algae *Symbiodinium* in a coral reef symbiosis. *Mol. Ecol.* **16**, 4849-4857.

Mayer, R. R., Cherry, J. H. and Rhodes, D. (1990). Effects of heat shock on amino acid metabolism of cowpea cells. *Plant Physiol.* **94**, 796-810.

Moran, R. (1982). Formulae for determination of chlorophyllous pigments extracted with N,N-dimethylformamide. *Plant Physiol.* **69**, 1376-1381.

Muscatine, L. and Cernichiari, E. (1969). Assimilation of photosynthetic products of zooxanthellae by a reef coral. *Biol. Bull.* **137**, 506-523.

Muscatine, L. and Hand, C. (1958). Direct evidence for the transfer of materials from symbiotic algae to the tissues of a coelenterate. *Proc. Natl. Acad. Sci. USA* **44**, 1259-1263.

Papina, M., Meziane, T. and van Woesik, R. (2003). Symbiotic zooxanthellae provide the host-coral *Montipora digitata* with polyunsaturated fatty acids. *Comp. Biochem. Physiol. B Biochem. Mol. Biol.* **135**, 533-537.

Papina, M., Meziane, T. and van Woesik, R. (2007). Acclimation effect on fatty acids of the coral *Montipora digitata* and its symbiotic algae. *Comp. Biochem. Physiol. B Biochem. Mol. Biol.* **147**, 583-589.

Pearcy, R. W. (1978). Effect of growth temperature on the fatty acid composition of the leaf lipids in *Atriplex lentiformis* (Torr.) Wats. *Plant Physiol.* **61**, 484-486.

Pernice, M., Meibom, A., Van Den Heuvel, A., Kopp, C., Domart-Coulon, I., Hoegh-Guldberg, O. and Dove, S. (2012). A single-cell view of ammonium assimilation in coral–dinoflagellate symbiosis. *ISME J.* **6**, 1314-1324.

Reynolds, J. M., Bruns, B. U., Fitt, W. K. and Schmidt, G. W. (2008). Enhanced photoprotection pathways in symbiotic dinoflagellates of shallow-water corals and other cnidarians. *Proc. Natl. Acad. Sci. USA* **105**, 13674-13678.

Rohwer, F., Seguritan, V., Azam, F. and Knowlton, N. (2002). Diversity and distribution of coral-associated bacteria. *Mar. Ecol. Prog. Ser.* **243**, 1-10.

Savchenko, T., Walley, J. W., Chehab, E. W., Xiao, Y., Kaspi, R., Pye, M. F., Mohamed, M. E., Lazarus, C. M., Bostock, R. M. and Dehesh, K. (2010). Arachidonic acid: an evolutionarily conserved signaling molecule modulates plant stress signaling networks. *Plant Cell* **22**, 3193-3205.

Smart, K. F., Aggio, R. B. M., Van Houtte, J. R. and Villas-Bôas, S. G. (2010). Analytical platform for metabolome analysis of microbial cells using methyl chloroformate derivatization followed by gas chromatography–mass spectrometry. *Nat. Protocols* **5**, 1709-1729.

Smith, D. J., Suggett, D. J. and Baker, N. R. (2005). Is photoinhibition of zooxanthellae photosynthesis the primary cause of thermal bleaching in corals? *Glob. Change Biol.* **11**, 1-11.

Smith, C. A., Want, E. J., O'Maille, G., Abagyan, R. and Siuzdak, G. (2006). XCMS: processing mass spectrometry data for metabolite profiling using nonlinear peak alignment, matching, and identification. *Anal. Chem.* **78**, 779-787.

Spann, N., Aldridge, D. C., Griffin, J. L. and Jones, O. A. H. (2011). Size-dependent effects of low level cadmium and zinc exposure on the metabolome of the Asian clam, *Corbicula fluminea*. *Aquat. Toxicol.* **105**, 589-599.

Starzak, D., Quinnell, R., Nitschke, M. and Davy, S. (2014). The influence of symbiont type on photosynthetic carbon flux in a model cnidarian–dinoflagellate symbiosis. *Mar. Biol.* **161**, 711-724.

Sunagawa, S., Choi, J., Forman, H. J. and Medina, M. (2008). Hyperthermic stress-induced increase in the expression of glutamate-cysteine ligase and glutathione levels in the symbiotic sea anemone *Aiptasia pallida*. *Comp. Biochem. Physiol. B Biochem. Mol. Biol.* **151**, 133-138.

Swanson, R. and Hoegh-Guldberg, O. (1998). Amino acid synthesis in the symbiotic sea anemone *Aiptasia pulchella*. *Mar. Biol.* **131**, 83-93.

Takahashi, S. and Murata, N. (2008). How do environmental stresses accelerate photoinhibition?. *Trends Plant Sci.* **13**, 178-182.

Tchernov, D., Gorbunov, M. Y., de Vargas, C., Narayan Yadav, S., Milligan, A. J., Häggblom, M. and Falkowski, P. G. (2004). Membrane lipids of symbiotic algae are diagnostic of sensitivity to thermal bleaching in corals. *Proc. Natl. Acad. Sci. USA* **101**, 13531-13535.

Tumanov, S., Bulusu, V. and Kamphorst, J. J. (2015a). Analysis of fatty acid metabolism using stable isotope tracers and mass spectrometry. In *Methods in Enzymology*, Vol. 561 (ed. M. M. Christian), pp. 197-217. New York: Academic Press.

Tumanov, S., Zubenko, Y., Greven, M., Greenwood, D. R., Shmanai, V. and Villas-Boas, S. G. (2015b). Comprehensive lipidome profiling of Sauvignon blanc grape juice. *Food Chem.* **180**, 249-256.

Viant, M. R. (2007). Metabolomics of aquatic organisms: the new omics on the block. *Mar. Ecol. Prog. Ser.* **332**, 301-306.

Viant, M. R. (2008). Recent developments in environmental metabolomics. *Mol. Biosyst.* **4**, 980-986.

Villas-Bôas, S. G., Mas, S., Åkesson, M., Smedsgaard, J. and Nielsen, J. (2005). Mass spectrometry in metabolome analysis. *Mass Spectrom. Rev.* **24**, 613-646.

Wakefield, T. S. and Kempf, S. C. (2001). Development of host- and symbiont-specific monoclonal antibodies and confirmation of the origin of the symbiosome membrane in a cnidarian–dinoflagellate symbiosis. *Biol. Bull.* **200**, 127-143.

Wang, J. and Douglas, A. (1998). Nitrogen recycling or nitrogen conservation in an alga–invertebrate symbiosis? *J. Exp. Biol.* **201**, 2445-2453.

Wang, J. T. and Douglas, A. E. (1999). Essential amino acid synthesis and nitrogen recycling in an alga–invertebrate symbiosis. *Mar. Biol.* **135**, 219-222.

Wang, L.-H., Lee, H.-H., Fang, L.-S., Mayfield, A. B. and Chen, C.-S. (2013). Fatty acid and phospholipid syntheses are prerequisites for the cell cycle of *Symbiodinium* and their endosymbiosis within sea anemones. *PLoS ONE* **8**, e72486.

Wang, L.-H., Chen, H.-K., Jhu, C.-S., Cheng, J.-O., Fang, L.-S. and Chen, C.-S. (2015). Different strategies of energy storage in cultured and freshly isolated *Symbiodinium* sp. *J. Phycol.* **51**, 1127-1136.

Weis, V. M. (2008). Cellular mechanisms of cnidarian bleaching: stress causes the collapse of symbiosis. *J. Exp. Biol.* **211**, 3059-3066.

Whitehead, L. F. and Douglas, A. E. (2003). Metabolite comparisons and the identity of nutrients translocated from symbiotic algae to an animal host. *J. Exp. Biol.* **206**, 3149-3157.

Wietheger, A., Fisher, P., Gould, K. and Davy, S. (2015). Sensitivity to oxidative stress is not a definite predictor of thermal sensitivity in symbiotic dinoflagellates. *Mar. Biol.* **162**, 2067-2077.

Xia, J., Psychogios, N., Young, N. and Wishart, D. S. (2009). MetaboAnalyst: a web server for metabolomic data analysis and interpretation. *Nucleic Acids Res.* **37**, W652-W660.

Xia, J., Mandal, R., Sinelnikov, I. V., Broadhurst, D. and Wishart, D. S. (2012). MetaboAnalyst 2.0: a comprehensive server for metabolomic data analysis. *Nucleic Acids Res.* **40**, W127-W133.